

Vibration behaviour of axially compressed cold-formed steel members

N. Silvestre[†] and D. Camotim[‡]

Department of Civil Engineering, IST/ICIST, Technical University of Lisbon, Av. Rovisco Pais, 1049-001 Lisboa, Portugal

(Received April 18, 2005, Accepted December 21, 2005)

Abstract. The objective of this work is to describe the main steps involved in the derivation of a GBT (*Generalised Beam Theory*) formulation to analyse the vibration behaviour of loaded cold-formed steel members and also to illustrate the application and capabilities of this formulation. In particular, the paper presents and discusses the results of a detailed investigation about the local and global free vibration behaviour of lipped channel simply supported columns. After reporting some relevant earlier GBT-based results dealing with the buckling and vibration behaviours of columns and load-free members, the paper addresses mostly issues concerning the variation of the column fundamental frequency and vibration mode nature/shape with its length and axial compression level. For validation purposes, some GBT-based results are also compared with values obtained by means of 4-node shell finite element analyses performed in the code ABAQUS.

Keywords: generalised beam theory (GBT); vibration analysis; buckling analysis; channel columns; column vibration; fundamental frequency; distortional modes; local-plate modes.

1. Introduction

It is a well-known fact that the proper assessment of the structural efficiency of a given cold-formed steel member requires in-depth information concerning its local (local-plate or distortional) and global buckling behaviour. In order to acquire it, one must inevitably identify the relevant buckling modes and evaluate the corresponding critical bifurcation stresses. Moreover, the above information also plays a crucial role in the development, validation and calibration of design rules and methodologies. Indeed, such methodologies are only rational and fully efficient if they can be based on reliable and physically sound models, a feature requiring a thorough knowledge concerning the member buckling and post-buckling behaviour.

Given the strong mathematical resemblance between the equations governing the stability and vibration behaviour of thin-walled members (they define similar eigenvalue problems), it is just logical to expect the vibration behaviour of cold-formed steel members to be equally susceptible to the cross-section in-plane and warping deformation. Since several commonly used applications of cold-formed steel members (e.g., storage rack structures) involve the simultaneous presence of significant

[†]Assistant Professor

[‡]Associate Professor, Corresponding author, E-mail: dcamotim@civil.ist.utl.pt

compressive applied loads and exposure to relevant dynamic actions (e.g., the effects due to heavy machines/vehicles or seismic activity), designers must be able to evaluate the corresponding dynamic response. Therefore, they must be equipped with efficient analytical and/or numerical tools to determine their vibration behaviour, possibly taking into account the influence of more or less relevant compressive internal forces.

Despite the available evidence concerning the relevance of the *local* vibration phenomena (e.g., Klaubruckner and Pryputniewicz 1995) and the influence of *compressive axial forces* on the *global* vibration behaviour (e.g., Hashemi and Richard 2000), the amount of research work that has been devoted to investigate the *local* vibration behaviour of *axially compressed* thin-walled members is still extremely scarce. In particular, it is worth mentioning the studies carried out by Ohga *et al.* (1998) and Okamura and Fukasawa (1998), who employed the semi-analytical finite strip method to assess the influence of axial compression on the local vibration behaviour of box and I-section members subjected to static and dynamic (periodic) forces. Nevertheless, one should also point out that this type of finite strip analyses can only be employed to study the vibration behaviour of “*simply supported*” thin-walled members (i.e., members with end-sections that are *pinned* in both directions and can warp freely - “fork-type” end conditions).

Generalised Beam Theory (GBT), which was originally developed by Schardt (1989) and has been extensively used by the authors in recent years (Camotim *et al.* 2004, 2005), incorporates both local and global cross-section deformation modes and has already been employed to perform free vibration analyses in the context of isotropic thin-walled members (e.g., Schardt and Heinz 1991). The objective of this paper is to present the derivation and illustrate the application and unique capabilities of an extension of the above GBT vibration formulation, which makes it possible to take into account the influence of the loads acting on the free vibrating member.

After a succinct description of the main concepts and procedures involved in deriving a GBT formulation to analyse the vibration behaviour of *loaded* thin-walled members, the content of the paper is focused on a particular application of this formulation: a detailed investigation about the local (local-plate or distortional) and global (flexural or flexural-torsional) free vibration behaviour of cold-formed steel lipped channel *simply supported columns*, i.e., uniformly compressed members with pinned and free-to-warp end sections. First, one must briefly report some GBT-based results dealing with (i) the buckling behaviour of columns and (ii) the vibration behaviour of load-free members, which have been recently determined (Silvestre and Camotim 2003) and are indispensable to interpret and discuss the column vibration analyses. Then, this paper addresses mostly issues that are concerned with an in-depth assessment of the variation of the column fundamental frequency and vibration mode nature/shape with its length and compression level, which is defined as a percentage of the relevant buckling loads. For validation purposes, some GBT-based results are compared with values obtained by means of finite element analyses, which are performed in the commercial code ABAQUS (HKS 2002) and employ fine meshes of 4-node isoparametric shell elements to discretise the lipped channel columns.

2. GBT governing equations

Due to space limitations, it is only possible to present here a brief description of the steps and procedures involved in the derivation of a GBT formulation making it possible to analyse the vibration behaviour of cold-formed steel members subjected to axial compression. It seems fair to say that this formulation combines the features of the ones previously developed by Schardt and his collaborators,

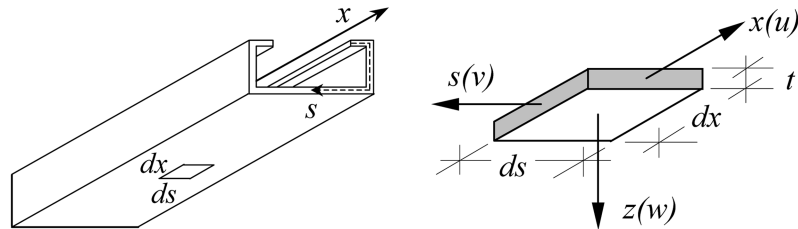


Fig. 1 Arbitrary open thin-walled member: geometry, coordinate system and displacement field

which were intended to perform linear stability and free vibration analyses in thin-walled profiles (e.g., Schardt 1989, Schardt and Heinz 1991, Schardt 1994).

Let us consider the prismatic member depicted in Fig. 1, which exhibits an open cross-section with an arbitrary shape and formed by n thin-walled plates (wall elements) that are rigidly connected along their common longitudinal edges. A *local* coordinate system (x, s, z) is adopted in each wall, where x and s define the corresponding mid-surface (longitudinal and transverse directions) and z is measured along the wall thickness t . When expressed in this coordinate system, the displacement field components are designated, respectively, as u, v and w .

In a GBT formulation, the displacement field at a given member cross-section is expressed as a linear combination of *deformation modes*, a feature making it possible to write the member equilibrium equations and boundary conditions in a rather unique and convenient fashion. Indeed, one is then capable of performing, in a very straightforward and natural way, a *modal* analysis of the cross-section deformed configuration, which provides a decisive contribution to a deeper and clearer understanding about the thin-walled member structural behaviour. In a member with n walls, a cross-section discretisation involving $n+1$ natural nodes (associated with the cross-section deformation due to warping) and m intermediate nodes (associated with the cross-section deformation due to wall bending alone, i.e., without any warping involved) leads to the identification of $n+m+1$ deformation modes: 4 global, $n-3$ distortional ones and m local-plate. For instance, Figs. 2(a)-(b) display cross-section discretisations that can be used to analyse the buckling or vibration behaviour of plain and lipped channel members, namely 9 ($n=4, m=5$) and 13 ($n=6, m=7$) nodes, respectively. Moreover, at the cross-section free edges one must include both a natural and an intermediate node (e.g., nodes 1 and 2) - the first concerns the lip free end warping and the second is related to its transversal (plate) bending.

The above discretisations lead to the identification of the following sets of *deformation modes*, which are depicted in Figs. 3 and 4: 9 modes (4 global and 5 local-plate), for the plain channel, and 13 modes (4 global, 2 distortional e 7 local-plate), for the lipped channel. Note that only the lipped channel



Fig. 2 (a) Plain and (b) lipped channel GBT cross-section discretisations

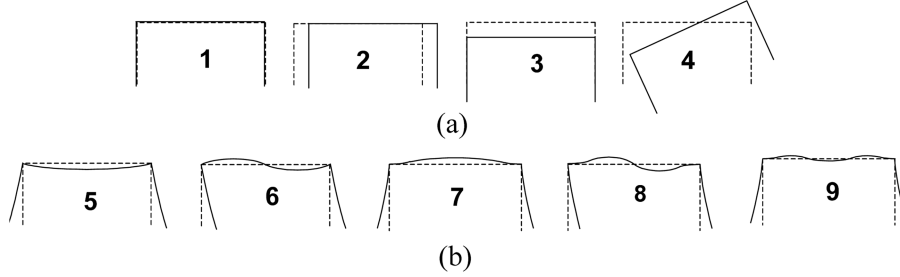


Fig. 3 Plain channel (a) global and (b) local-plate deformation mode shapes

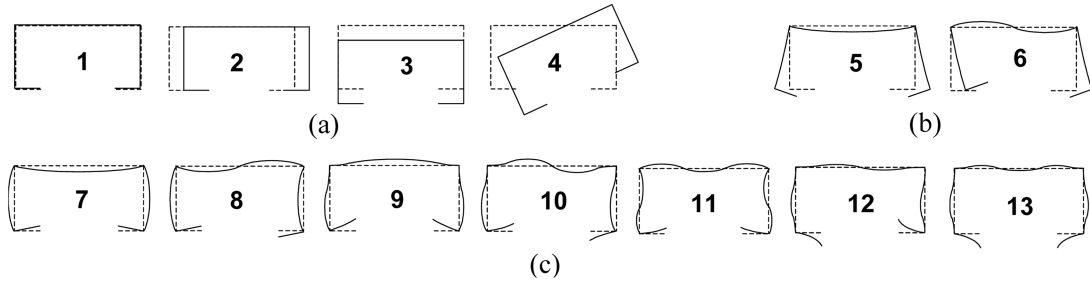


Fig. 4 Lipped channel (a) global, (b) distortional and (c) local-plate deformation mode shapes

exhibits distortional modes - modes **5** and **6**. Since it is an unbranched cross-section with just three walls (i.e., four natural nodes), the plain channel does not exhibit distortional deformation modes. Certain deformed configurations of plain channel members are sometimes designated as “distortional” due to the fact that they exhibit both (i) fold line motions (due to warping displacements) and (ii) cross-section in-plane deformation. However, these two features originate in distinct phenomena: (i) the fold line motions (associated with warping displacements), due solely to *global modes* (bending and/or torsion), and (ii) the cross-section in-plane deformation, due exclusively to *local-plate modes*. Thus, these so-called “distortional modes” are, in fact, *mixed local-plate/global modes*. For more detailed explanations about the distortional mode mechanics, the interested reader is referred to works by Schardt (1989) and Adány (2004).

Following the application of Hamilton’s Principle, one is led to a system of equilibrium equations given by (Silvestre 2005)

$$C_{ik}\phi_{k,xxxx} - D_{ik}\phi_{k,xx} + B_{ik}\phi_k - \mathbf{a}_B \lambda W_p^0 X_{pik}\phi_{k,xx} - \mathbf{a}_v \omega^2 (R_{ik}\phi_k - Q_{ik}\phi_{k,xx}) = 0 \quad (1)$$

where (i) $\phi_k(x)$ is the amplitude function associated with *deformation mode k*, defined along the member length ($0 \leq x \leq L$), (ii) W_p^0 is the *pre-buckling* normal stress resultant corresponding to *deformation mode p*, deemed uniform (i.e., independent of x), (iii) λ is an applied load parameter and (iv) ω is a frequency parameter, concerning the member harmonic free vibration. The end support conditions of the member can be written as

$$(W_i^\tau + \mathbf{a}_B W_p^0 X_{pik}\phi_{k,x} - \mathbf{a}_v \omega^2 Q_{ik}\phi_{k,x}) \delta\phi_i \Big|_0^L = 0 \quad W_i^\sigma \delta\phi_{i,x} \Big|_0^L = 0 \quad (2)$$

where

$$W_i^\sigma = C_{ik} \phi_{k,xx} + D_{ik}^2 \phi_k \quad W_i^\tau = -C_{ik} \phi_{k,xxx} + (D_{ik}^1 - D_{ik}^2) \phi_{k,x} \quad (3)$$

are generalised internal forces due to the *normal* and *shear* stresses related to deformation mode k and acting at the member end sections. If one makes (i) $\mathbf{a}_B=1$ and $\mathbf{a}_V=0$, (ii) $\mathbf{a}_B=0$ and $\mathbf{a}_V=1$ or (iii) $\mathbf{a}_B=\psi$ ($0 < \psi \leq 1$) and $\mathbf{a}_V=1$, Eqs. (1) and (2) define a linear eigenvalue problem associated, respectively, with a member (i) buckling analysis, (ii) free vibration analysis of load-free members and (iii) free vibration analysis of loaded members (i.e., acted by generalised internal forces W_p^o). In the last case, note that the value of W_p^o is known *a priori* and ω^2 are the problem eigenvalues - it is also worth noting that the generalized internal forces W_p^o (uniform along the member length) can be either (i) axial compressive forces ($W_1^o=N$), (ii) major or minor axis bending moments ($W_2^o=M_I$ or $W_3^o=M_{II}$), (iii) bi-moments ($W_4^o=B$) or (iv) any combination of them.

Finally, the tensorial quantities appearing in Eqs. (1)-(3) are given by the expressions

$$C_{ik} = E \int_b \left(t u_i u_k + \frac{1}{12} t^3 w_i w_k \right) ds \quad B_{ik} = \frac{E}{12(1-\nu^2)} \int_b t^3 w_{i,ss} w_{k,ss} ds \quad (4)$$

$$D_{ik} = G \int_b \frac{1}{3} t^3 \left(w_{i,s} w_{k,s} - \frac{\nu}{2(1-\nu)} (w_i w_{k,ss} + w_k w_{i,ss}) \right) ds \quad (5)$$

$$X_{pik} = \frac{E}{C_{pp}} \int_b t u_p (v_i v_k + w_i w_k) ds \quad (6)$$

$$Q_{ik} = \rho \int_b \left(t u_i u_k + \frac{1}{12} t^3 w_i w_k \right) ds \quad R_{ik} = \rho \int_b \left(t (v_i v_k + w_i w_k) + \frac{1}{12} t^3 w_{i,s} w_{k,s} \right) ds \quad (7)$$

where the steel properties E , G , ν and ρ are the Young's modulus, shear modulus, Poisson's ratio and mass density, respectively. As for the matrices associated with these tensors, it is worth noting that:

- (i) $[C_{ik}]$, $[D_{ik}]$ and $[B_{ik}]$ are stiffness matrices related to generalized warping, torsion and transverse bending (*cross-section in-plane deformation*), respectively. The first two terms of tensor C_{ik} stand for the cross-section primary and secondary warping components.
- (ii) $[X_{ik}]_p$ is the geometric stiffness matrix, which accounts for the influence of the interaction between the normal stresses (stemming from the pre-buckling displacements associated with deformation mode p) and the in-plane cross-section deformations (strains).
- (iii) $[Q_{ik}]$ and $[R_{ik}]$ are mass matrices incorporating the effects of the mass (inertia) forces concerning, respectively, the *out-of* and *in-plane* cross-section displacements. The first and second terms in the tensor components Q_{ik} and R_{ik} always correspond to translational and rotational inertia forces. It should still be pointed out that the components of Q_{ik} and C_{ik} satisfy the relationship $Q_{ik}/\rho = C_{ik}/E$, which means that they are directly proportional.

Because the equilibrium equations (Eq. (1)) are normally *coupled*, it is convenient to perform the simultaneous diagonalisation of matrices $[C_{ik}]$ and $[B_{ik}]$, an operation that involves the solution of a standard eigenvalue problem and makes it possible to take full advantage of all the GBT capabilities. Note also that, although matrix $[D_{ik}]$ is not diagonal (*first order coupling*), its off-diagonal components are rather small (when compared with the corresponding diagonal components) and can be neglected, which amounts to including an "approximate" diagonal matrix $[D_{ik}]$ in the analysis. However, due to the presence of the non-null off-diagonal components of matrices $[X_{ik}]_p$ (*second order coupling*) and $[R_{ik}]$ (*dynamic coupling*), system (1) is invariably coupled, which means that the member buckling and

vibration modes involve, at each cross-section, linear combinations of the GBT deformation modes. Therefore, after having solved the system (1) and determined the modal amplitude functions $\phi_k(x)$, the displacement field associated with a given buckling or vibration mode is defined by

$$\begin{aligned} u(x,s) &= u_k(s) \phi_{k,x}(x) \\ v(x,s) &= v_k(s) \phi_k(x) \\ w(x,s) &= w_k(s) \phi_k(x) \end{aligned} \quad (8)$$

where functions $u_k(s)$, $v_k(s)$ and $w_k(s)$, which are known *a priori*, provide the displacement shapes (profiles) corresponding to *deformation mode k*.

The illustration of the proposed GBT formulation presented here concerns exclusively its application to analyse the vibration behaviour of *columns* (i.e., axially compressed members) - in other words, $W_1^o = N$ (member axial compression) is the only non-null generalised internal force dealt with in this work. Note, however, that the authors have recently published similar results dealing with FRP composite *columns* (Silvestre and Camotim 2005a, 2006) and *beams* (members under uniform major axis bending – Silvestre and Camotim 2005b, 2006).

In the following sections, one presents and briefly discusses recent GBT-based buckling and vibration results concerning cold-formed steel lipped channel members, namely the (i) buckling behaviour of columns, (ii) the vibration behaviour of load-free members and, to conclude, (iii) the vibration behaviour of columns. It is worth noting that these results have been obtained on the basis of the GBT cross-section discretisation shown in Fig. 2(b) and that only simply supported members (i.e., members pinned and free-to-warp end sections) are analysed, which means that both the *exact* buckling and vibration mode shapes are *sinusoidal*. Moreover, note also that the member cross-section dimensions, material properties and mass density employed in the analyses are the following: $b_w=100$ mm (web width), $b_f=60$ mm (flange width), $b_l=10$ mm (lip width), $t=2$ mm (wall thickness), $E=210$ MPa, $\nu=0.3$ and $\rho=7.85 \times 10^{-3}$ g/mm³.

3. Column buckling behaviour

In order to investigate the vibration behaviour of loaded lipped channel columns, one must begin by studying their buckling behaviour. The reason for this is that one always performs vibration analyses of columns subjected to axial loads that correspond to a certain *percentage* of its *critical buckling load* (P_{cr}). The curves displayed in Fig. 5(a) make it possible to assess the variation, with the column length L (in logarithmic scale), of (i) the bifurcation loads associated with single, two and three-wave buckling modes ($P_{b,1}$, $P_{b,2}$ and $P_{b,3}$) and (ii) the “true” critical load ($P_{cr} = \min\{P_{b,1}; P_{b,2}; P_{b,3}\}$ ¹). On the other hand, the diagrams shown in Figs. 5(b) and 5(c) provide the variation of the participation of the relevant GBT deformation modes in the column buckling modes corresponding to P_{cr} and $P_{b,1}$ (the lipped channel deformation mode shapes are depicted in Fig. 4). In the former case, one should point out that, in order to provide valuable information concerning the number of (half) waves associated with the participation of a given deformation mode, the number identifying this mode is either not underlined (*single wave*), underlined once (2 waves) or underlined twice (3 waves). From the observation of the

¹It can be shown that, for this particular column geometry, no *critical* buckling mode exhibits more than three waves.

results presented in Figs. 5(a)-(c), it possible to draw the following conclusions:

- (i) For $L < 75$ cm, the *single-wave* buckling modes combine only three *local* deformation modes, namely modes **5**, **7** and **9** (Fig. 5(c)). Inside this length range, the curve $P_{b,1}$ vs. L exhibits two local minima, corresponding to buckling in (i₁) a *local-plate* mode (LPM - mode **7** plus a bit of modes **5** and **9**) and (i₂) a *distortional* mode (DM - mode **5** plus a bit of mode **7**). They are associated with critical bifurcation values $P_{cr,LP}=192.1$ kN ($L=8$ cm) and $P_{cr,D}=154.4$ kN ($L=70$ cm) - note that, in this particular case, one has $P_{cr,D} < P_{cr,LP}$. For $14 < L < 24$ cm, there is a smooth transition between LPM and DM, which corresponds to the occurrence of *mixed local-plate/distortional* modes (LPDM - modes **5** and **7**).
- (ii) For $75 < L < 250$ cm, the single-wave buckling modes combine two global and one local GBT deformation modes, namely modes **2** (major axis flexure), **4** (torsion) and **6** (distortion),

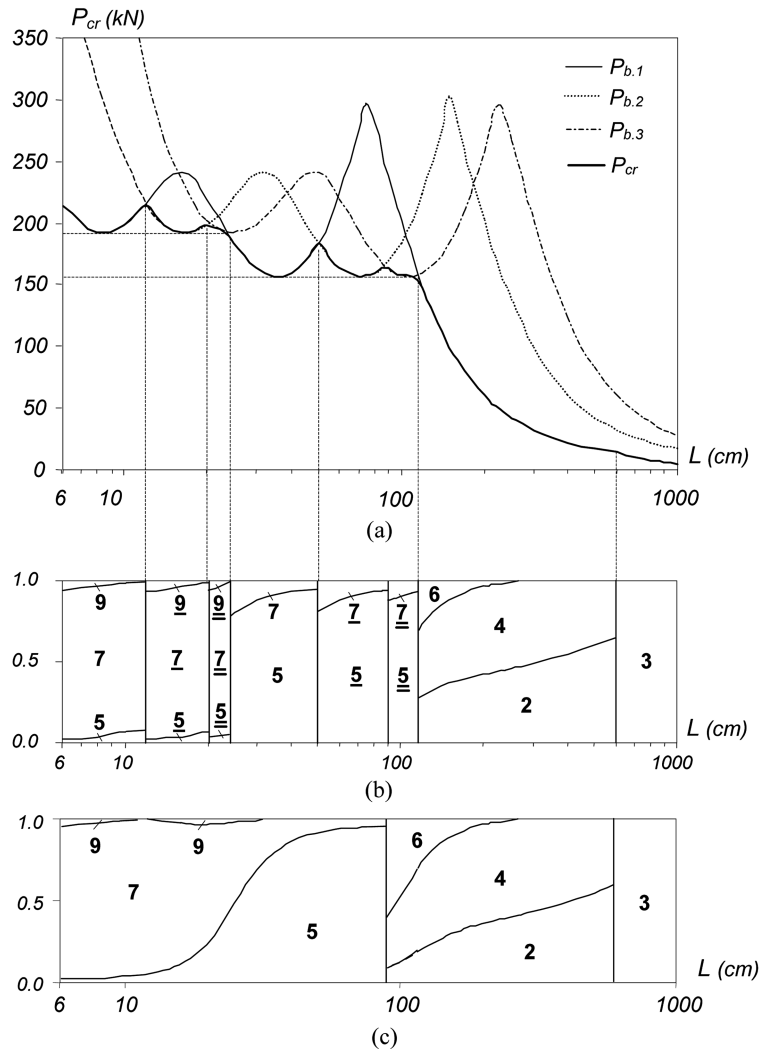


Fig. 5 Column buckling behaviour: (a) variation of $P_{b,1}$, $P_{b,2}$, $P_{b,3}$, P_{cr} with L and GBT modal participation in the (b) "true" and (c) single-wave critical buckling modes

which explains the designation *flexural-torsional-distortional* (FTDM). The participation of mode 6 gradually decreases and vanishes for $L \approx 250$ cm. Then, for $250 < L < 600$ cm, the buckling modes combine only modes 2 and 4 - the classical flexural-torsional modes (FTM). Finally, the very long columns ($L > 600$ cm) buckle in purely flexural modes (FM - mode 3, i.e., minor axis flexure). It is still worth noting that (ii₁) the curve $P_{b,1}$ vs. L continuously decreases for $L > 75$ cm and (ii₂) the transitions between the DM-FTDM and FTM-FM length ranges are abrupt: the participation of one or more GBT deformation modes ceases suddenly.

- (iii) Since the curves $P_{b,2}$ vs. L and $P_{b,3}$ vs. L are obtained by mere horizontal translations of the curve $P_{b,1}$ vs. L , the “true” column buckling modes combine exactly the same set of GBT deformation modes participating in the single-wave ones. The only difference resides in the fact that the number of waves associated with some of these modes changes for certain length ranges (when the curve P_{cr} vs. L does not coincide with $P_{b,1}$ vs. L - see Fig. 5(a)). Indeed, the “true” column buckling modes exhibit more than one wave for (iii₁) $12 < L < 20$ cm (two-wave LPM), (iii₂) $20 < L < 24$ cm (three-wave LPM), (iii₃) $50 < L < 90$ cm (two-wave DM) and (iii₄) $90 < L < 115$ cm (three-wave DM).

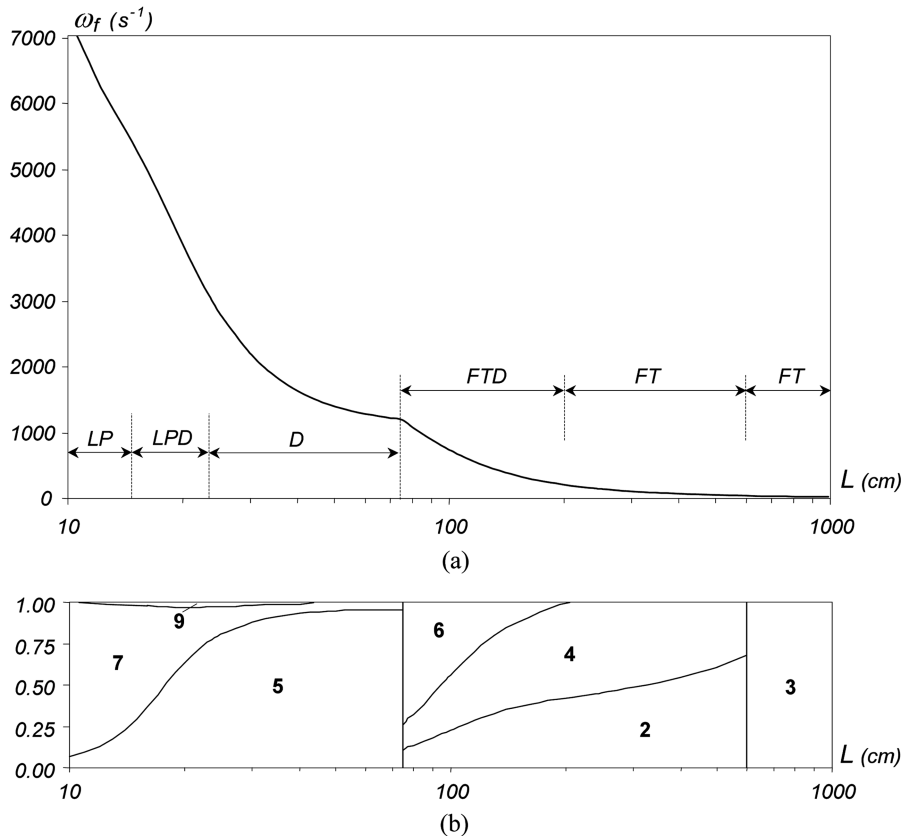


Fig. 6 Load-free member vibration behaviour: (a) variation of ω_f with L and (b) GBT modal participation in the fundamental vibration mode

4. Vibration behaviour of load-free members

The curves in Fig. 6(a) provide the variation, with length L (in logarithmic scale), of the member fundamental frequency ω_f which is always associated with *single-wave* vibration modes². As for the diagram presented in Fig. 6(b), it makes it possible to assess the variation of the GBT modal participation in the column fundamental vibration mode. A comparison between the results presented in Figs. 5(a), 5(c), 6(a) and 6(b) leads to the following conclusions:

- (i) In spite of the different characteristics exhibited by the curves $P_{b,1}$ vs. L and ω_f vs. L shown in Figs. 5(a) and 6(a) (e.g., the latter has no local minima), the GBT modal participation diagrams displayed in Figs. 5(c) and 6(b) are *identical*³, which means that the shapes of the (i₁) column critical single-wave buckling modes and (i₂) load-free member fundamental vibration modes *coincide*, regardless of the length value L . Silvestre (2005) recently proved this coincidence and also showed that the exact ω_f and $P_{b,1}$ values must satisfy the relation

$$\omega_f = \frac{\pi}{L} \sqrt{\frac{P_{b,1}}{\rho A}} \quad (9)$$

where A is the member cross-section area. This relation is always universally valid for simply supported members, i.e., it applies to any buckling/vibration mode shape (local-plate, distortional, global). In the context of global (bending, torsion) vibration/buckling analyses, several authors (e.g., Wittrick 1985, Roberts 1987) have verified that this relation holds true. However, as far as local vibration/buckling analyses are concerned, only one work has been found (Okamura and Fukasawa 1998) - these authors employed the semi-analytical finite strip method to confirm that the *local* buckling and vibration modes exhibit equal shapes, regardless of the member length. Finally, one should also mention that Eq. (9) has a more general form,

$$\omega_{n,nw} = \frac{n_w \pi}{L} \sqrt{\frac{P_{b,nw}}{\rho A}} \quad (10)$$

where $P_{b,nw}$ and $\omega_{n,nw}$ are bifurcation loads and natural frequencies corresponding to buckling and vibration modes with an arbitrary number of waves n_w .

- (ii) The content of the above item (i) automatically implies that all the conclusions drawn in the previous subsection, concerning the column single-wave buckling behaviour, also apply to the fundamental vibration behaviour of load-free members. Therefore, there is no need to further characterise the latter.

5. Column vibration behaviour

Finally, one presents and thoroughly discusses the results of a detailed study concerning the vibration behaviour of cold-formed steel lipped channel simply supported columns, which is the main aim of this paper. Once again, all the columns analysed display the geometrical and material properties given in the previous section. Note also that, for validation purposes, some GBT-based fundamental frequencies and

²Note the qualitative difference with respect to the column critical buckling behaviour: inside certain length ranges, the "true" critical buckling modes exhibit two or three waves.

³Note that, while the diagram in Fig. 6(b) starts at $L=10$ cm, the one in Fig. 5(c) starts at $L=6$ cm.

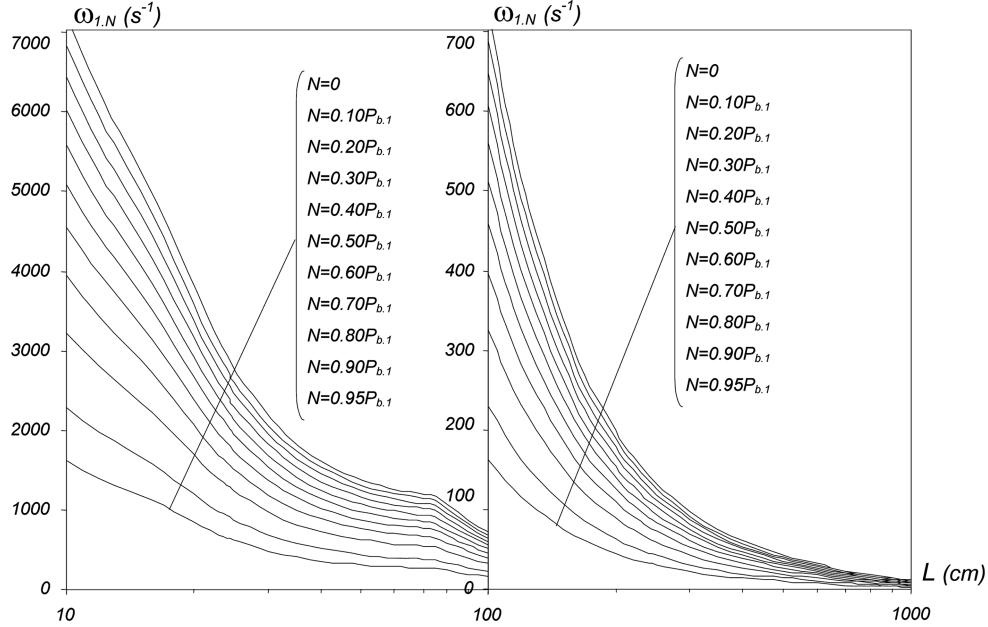


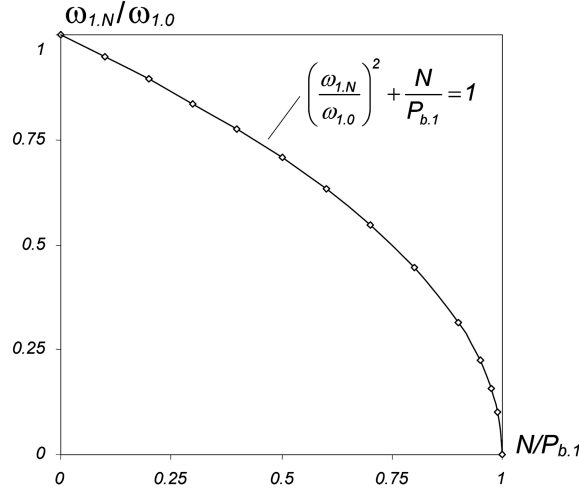
Fig. 7 Variation of the natural frequency value $\omega_{1,N}$ with the column length L and axial force N

vibration mode shapes are compared with the values yielded by shell finite element analyses, performed in the code ABAQUS (HKS 2002) and adopting fine meshes of 4-node shell elements (S4 elements) to discretise the columns.

The curves given in Fig. 7 concern the vibration behaviour of simply supported columns and make it possible to assess how the natural frequency associated with a single-wave sinusoidal vibration mode ($\omega_{1,N}$) varies with the column length and axial (compressive) force level N^4 . Ten axial force levels are considered, each one corresponding to a different percentage of the column critical single-wave buckling load $P_{b,1}$ (Fig. 5(a)). For clarity and comparison purposes, one uses different vertical scales ($L \leq 100$ cm and $L > 100$ cm) and the curve related to the vibration behaviour of the load-free member ($N = 0 - \omega_{f,0}$) is also included - recall that this curve was already shown in Fig. 6(a) ($\omega_f \equiv \omega_{f,0}$). The observation of this set of curves prompts the following comments:

- (i) The various curves $\omega_{1,N}(L)$ exhibit very similar shapes, which means that it is possible to relate each of them to $\omega_{1,0}(L)$ by means of a multiplicative factor $\alpha \leq 1$, so that one may write $\omega_{1,N}(L) = \alpha \omega_{1,0}(L)$. Note that, if $N = P_{b,1}$, one obviously has $\alpha = 0$.
- (ii) As it would be logical to expect, in view of the coincidence between the shapes of the single-wave (ii₁) column critical buckling modes and (ii₂) load-free member vibration modes, the fundamental vibration mode configurations of the load-free members (shown in Fig. 6(b)) and axially compressed members (not shown in this paper) also *coincide*.
- (iii) For any given L , the variation of $\omega_{1,N}$ with N is non-linear: for equal ΔN increments, the frequency drop $\Delta \omega_{1,N}$ decreases as N grows. Moreover, it was found that the curve shown in Fig. 8, which provides the variation of the ratio $\omega_{1,N}/\omega_{1,0}$ with the normalised axial force level

⁴In the overwhelming majority of the cases, $\omega_{1,N}$ is, actually, the column fundamental frequency $\omega_{f,N}$. However, there are a few exceptions, which will be dealt with further ahead in the paper.


 Fig. 8 Variation of $\omega_{1,N}/\omega_{1,0}$ with $N/P_{b,1}$

$N/P_{b,1}$, is applicable to any length value L . On the basis of the previous two facts, one may conclude that the above multiplicative factor α (iii₁) depends non-linearly on N and (iii₂) is independent of L . By observing Fig. 8, one notices that, for $0 < N < 0.50P_{b,1}$, $\Delta\omega_{1,N}$ is fairly (inversely) proportional to ΔN . For $N > 0.50P_{b,1}$, on the other hand, the curve is clearly non-linear and exhibits a growing negative slope, which becomes very steep for $N > 0.80P_{b,1}$.

In order to explain and quantify the above statements, let us rewrite Eq. (1), in matrix form and under the assumption of a *single-wave* sinusoidal vibration mode (an exact solution):

$$\left[C_{ik} \left(\frac{\pi}{L} \right)^4 + D_{ik} \left(\frac{\pi}{L} \right)^2 + B_{ik} \right] - \left(\frac{N}{\rho A} \left(\frac{\pi}{L} \right)^2 + \omega_{1,N}^2 \right) R_{ik} = 0 \quad (11)$$

Then, taking into account that N only appears in the second term of Eq. (11), it becomes clear that the lowest eigenvalues associated with $N \neq 0$ ($\omega_{1,N}$) and $N=0$ ($\omega_{1,0}$) are related by

$$\omega_{1,N}^2 + \frac{N}{\rho A} \left(\frac{\pi}{L} \right)^2 = \omega_{1,0}^2 \quad (12)$$

or, after incorporating the Eq. (9), where $\omega_f \equiv \omega_{1,0}$, into Eq. (12), by

$$\left(\frac{\omega_{1,N}}{\omega_{1,0}} \right)^2 + \frac{N}{P_{b,1}} = 1 \quad (13)$$

This equation provides a *direct* relationship between the frequency ratio $\omega_{1,N}/\omega_{1,0}$ and the column normalised axial force $N/P_{b,1}$, which does not depend explicitly on the column length or cross-section geometry (the influence of these parameters is implicitly included via the $\omega_{1,0}$ and $P_{b,1}$ values). Then, one immediately realises that the value of the multiplicative factor α (i.e., the shape of the curve depicted in Fig. 8) is given by the *exact* expression

$$\alpha = \frac{\omega_{1,N}}{\omega_{1,0}} = \sqrt{1 - \frac{N}{P_{b,1}}} \quad (14)$$

As mentioned before, this last expression was derived under the assumption that both the column buckling modes and the load-free member vibration modes have single-wave sinusoidal shapes. While the latter assertion has been shown to be always valid for the fundamental vibration modes, it is also a well-known fact that the same does not apply to all the column “true” critical buckling modes. Indeed, some columns with intermediate lengths were found to buckle in two or three-wave modes (see Figs. 5(a)-(b)). Thus, it is quite important to investigate and characterise the fundamental vibration behaviour of such columns. To attain this goal, let us start by considering the results presented in Figs. 9(a)-(b) and 10(a)-(e). The curves shown in the first two figures provide the variation, with the column length L , of the *fundamental* frequencies $\omega_{f,N}$ ($N \neq 0$ - seven axial force levels) and $\omega_{f,0}$ ($N=0$) and, in order to enable a direct comparison, also the column *single-wave* ($P_{b,1}$) and “*true*” (P_{cr}) critical bifurcation loads (already presented in Fig. 5(a)). It is also worth noting that (i) one uses again different vertical scales ($L \leq 50$ cm and $L > 50$ cm this time) and (ii) the column axial forces are now normalised with respect to P_{cr} (instead of $P_{b,1}$, as in Fig. 7). As for the GBT modal participation diagrams shown in Fig. 10, they correspond to columns acted by different axial forces and make it possible to assess how the fundamental vibration mode shape varies with N . The observation of the results displayed in Figs. 9(a)-(b) and 10 prompts the following comments:

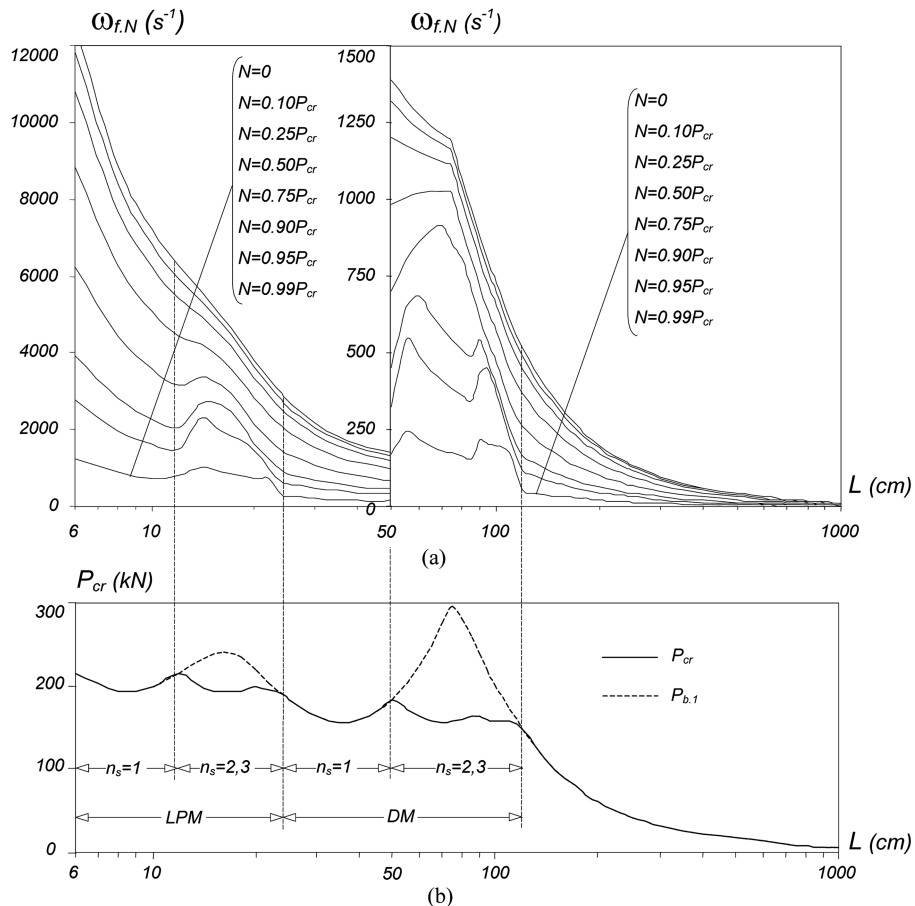


Fig. 9 Variation of (a) the fundamental frequency $\omega_{f,N}$ with L and N and (b) $P_{b,1}$ and P_{cr} with L

- (i) The shapes of the *fundamental* frequency curves $\omega_{f,N}(L)$ are clearly different from the ones depicted in Fig. 7 and concerning *single-wave* vibration ($\omega_{1,N}(L)$). Moreover, the shape of $\omega_{f,N}(L)$ varies considerably with the value of N .
- (ii) However, a closer look shows that the portions of the $\omega_{f,N}(L)$ curves corresponding to length ranges inside which one has $P_{cr}=P_{b,1}$ (i.e., a *single-wave* column “true” critical buckling mode) are associated with single-wave fundamental vibration modes (i.e., $\omega_{f,N} \equiv \omega_{1,N}$) and, thus, *continue* to be related by Eq. (14). Such length ranges are well identified in Fig. 9(b) and are: $L < 12$ cm (LPM), $24 < L < 50$ cm (DM) e $L > 115$ cm (FTDM, FTM and FM).
- (iii) Concerning the length ranges inside which one has $P_{cr} \neq P_{b,1}$ (i.e., *two* or *three-wave* column

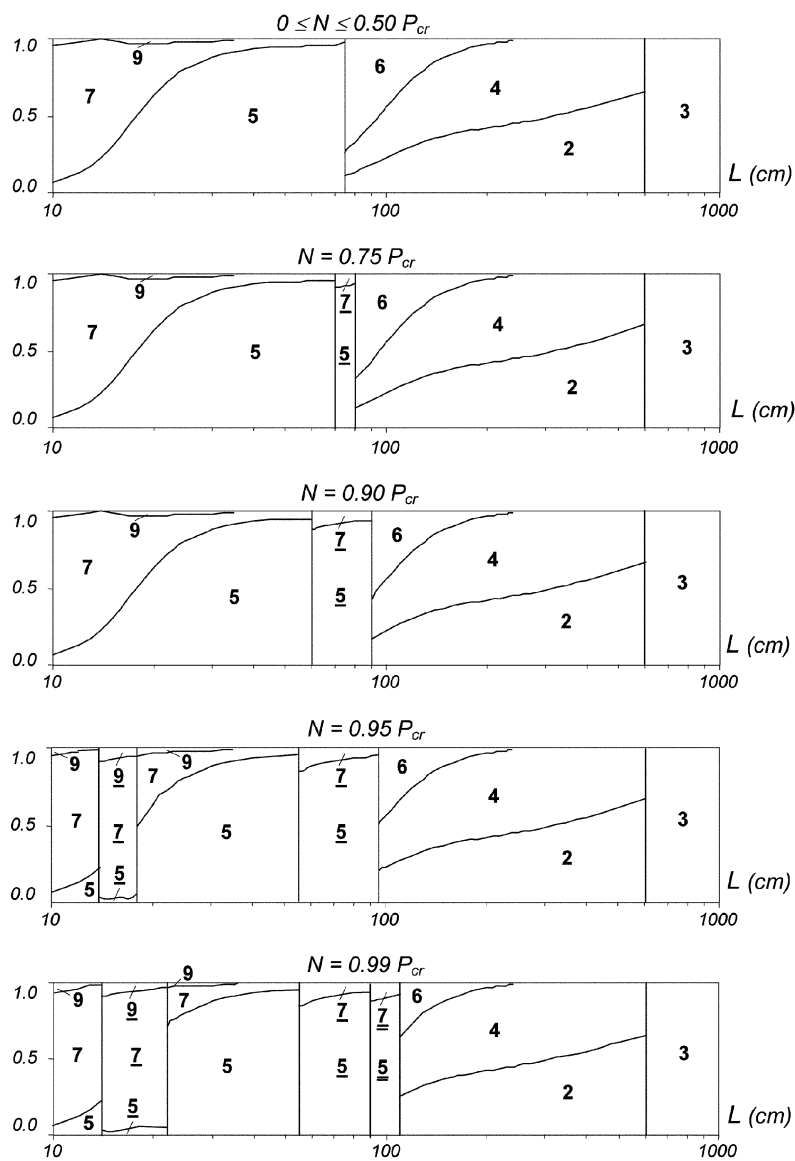


Fig. 10 GBT modal participation in the column fundamental vibration mode

“true” critical buckling modes - $12 < L < 24$ cm and $50 < L < 115$ cm), Eq. (14) is no longer valid and further investigation is necessary. In particular, one notices that, within these length ranges, the $\omega_{f,N}(L)$ curves cease to decrease monotonically and there is a clearly visible shape variation with N . Moreover, one also observes that, as N increases, the $\omega_{f,N}(L)$ curves become progressively less “smooth” - for very large axial forces, they may even exhibit quite pronounced and sudden *slope reversals*.

- (iv) The diagrams presented in Fig. 10 show that, provided that the axial force N is sufficiently high, the fundamental vibration modes of columns with certain length values (all located inside the $12 < L < 24$ cm and $50 < L < 115$ cm intervals) exhibit two or three waves.
- (v) The diagrams in Fig. 10 show that, when $P_{cr} \neq P_{b,1}$, the column fundamental vibration mode wave number changes with N . It varies between one and the number of waves in the column critical buckling mode (two or three, in this particular case). It appears that the value of N corresponding to a wave number change depends on the percentage difference between P_{cr} and $P_{b,1}$ (i.e., a ratio $P_{cr}/P_{b,1}$ decrease lowers the N value associated with the change).
- (vi) In other words, as N increases, the column fundamental vibration wave number “travels” between one and the number of waves of the column critical buckling mode. On the basis of finite strip vibration analyses, Ohga *et al.* (1998) reached a similar conclusion.

Finally, the curves shown in Fig. 11 provides the variation of $\omega_{f,N}/\omega_{f,0}$ with $N/P_{b,1}$, for columns with lengths $L=16$ cm ($12 < L < 24$ cm) and $L=75$ cm ($50 < L < 115$ cm), which buckle in two-wave local-plate and distortional modes, respectively. Because N is normalised with respect to $P_{b,1}$, these two curves can be directly compared with the one concerning the ratio $\omega_{1,N}/\omega_{1,0}$ (dashed curve - already depicted in Fig. 8). Such a comparison leads to the following remarks:

- (i) For “sufficiently low” N values, the $\omega_{f,N}/\omega_{f,0}$ and $\omega_{1,N}/\omega_{1,0}$ curves virtually coincide, which means that the relation (14) is still applicable (even if one has $P_{cr} \neq P_{b,1}$).
- (ii) The N value associated with the “separation” between the curves $\omega_{f,N}/\omega_{f,0}$ and $\omega_{1,N}/\omega_{1,0}$ is considerably lower for the column buckling in a DM ($L=75$ cm) than for the one buckling in a LPM ($L=16$ cm) - $N/P_{b,1} \approx 0.28$ vs. $N/P_{b,1} \approx 0.72$. Most likely, it will be possible to find a

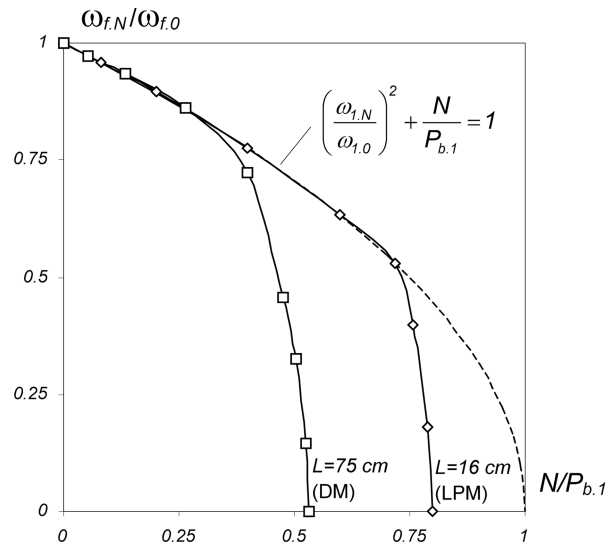


Fig. 11 Variation of $\omega_{f,N}/\omega_{f,0}$ with $N/P_{b,1}$ for columns with $L=16$ cm (LPM) and $L=75$ cm (DM)

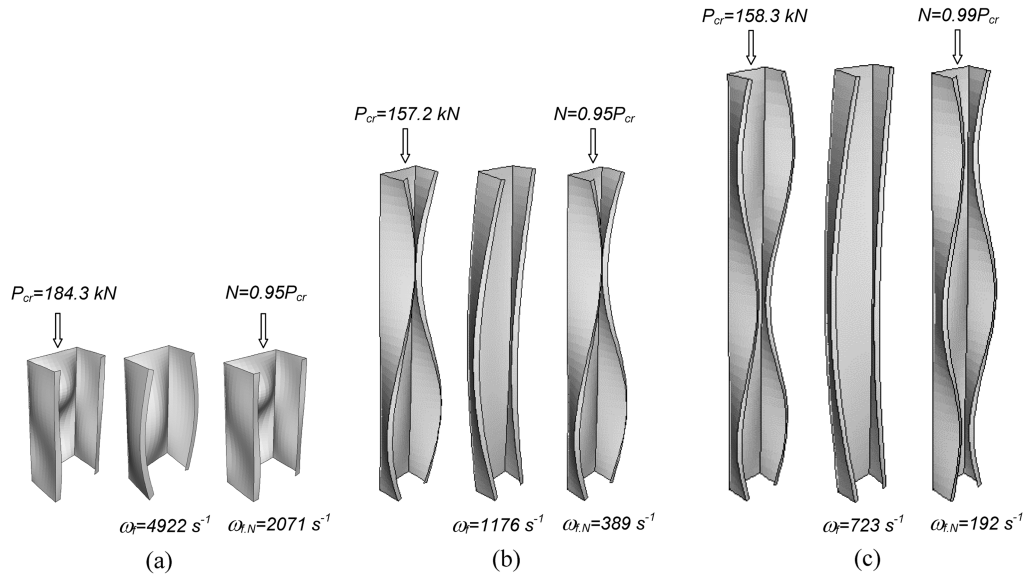


Fig. 12 FEM-based results concerning columns with (a) $L=16$ cm, (b) $L=75$ cm and (c) $L=100$ cm

correlation between this axial force “separation level” and the ratio $P_{cr}/P_{b,1}$ - note that one has $P_{cr}/P_{b,1} \approx 0.53$ vs. $P_{cr}/P_{b,1} \approx 1.80$, respectively for the $L=75$ and $L=16$ cm columns.

(iii) When the $N/P_{b,1}$ “separation value” is higher ($L=16$ cm), the ensuing variation (decrease) of $\omega_{f,N}/\omega_{f,0}$ with $N/P_{b,1}$ is more drastic, in the sense that the corresponding curve is “steeper”.

Finally, for validation purposes, Fig. 12 shows numerical results yielded by finite element analyses performed in the code ABAQUS (HKS 2002) and adopting S4 shell elements to discretise the columns. They concern highly compressed columns with $L=16$ cm, $L=75$ cm and $L=100$ cm and consist of their P_{cr} , $\omega_{f,0}$ and $\omega_{f,N}$ values and corresponding critical buckling and fundamental vibration mode shapes. Concerning the FE meshes, one adopted a cross-section mid-line discretisation comprising 32 finite elements and a longitudinal discretisation involving 20 ($L=16$ cm) and 40 ($L=75$ and $L=100$ cm) finite elements - this led to meshes with 640 ($L=16$ cm) and 1280 finite elements ($L=75$ and $L=100$ cm). One observes that there exists an excellent agreement between the GBT and FEM-based results: indeed, the errors never exceed 1.7% and the FEM-based buckling and vibration mode shapes fully confirm the conclusions drawn from the GBT analyses.

6. Conclusions

The derivation of a GBT formulation to analyse the vibration behaviour of *loaded* cold-formed steel members was first described. In order to illustrate its application and capabilities, the paper then presented and discussed the results of a detailed study concerning the local and global free vibration behaviour of lipped channel simply supported columns. For validation, some GBT-based results were also compared with values yielded by ABAQUS shell finite element analyses.

The analysis of the GBT-based results obtained led to the following main conclusions:

- (i) The shapes of column (i₁) critical single-wave buckling mode and (i₂) fundamental vibration mode are fully identical.

- (ii) When the axial force N increases, the column fundamental frequency ω_{fN} (almost always) decreases and the associated vibration mode shape tends to the critical buckling mode one.
- (iii) For *low* axial force levels ($N < 0.25P_{cr}$), the ω_{fN}/ω_{f0} decrease is fairly proportional to the $N/P_{b,1}$ increase. On the other hand, *high* axial force levels ($N > 0.50P_{cr}$) lead to a rather large drop in the column fundamental frequency ω_{fN} .
- (iv) In columns with *single-wave* critical buckling modes, it is possible to derive *exact* analytical expressions relating the ω_{fN} and ω_{f0} values, which involves only N and the critical load P_{cr} .

References

- Ádány S. (2004). "Buckling mode classification of members with open thin-walled cross-sections by using the finite strip method", Research Report, Department of Civil Engineering, Johns Hopkins University, Baltimore.
- Camotim, D., Silvestre, N., Gonçalves, R. and Dinis, P. B. (2004), "GBT analysis of thin-walled members: New formulations and applications", *Thin-Walled Structures: Recent Advances and Future Trends in Thin-Walled Structures Technology* (International Workshop, Loughborough, June 25), J. Loughlan (Ed.), Canopus Publishing, Bath, 137-168.
- Camotim, D., Silvestre, N. and Dinis, P. B. (2005), "Numerical analysis of cold-formed steel members", *Int. J. of Steel Structures*, **5**(1), 63-78.
- Hashemi, S. M. and Richard, M. J. (2000), "Free vibrational analysis of axially loaded bending-torsion coupled problems: A dynamic finite element", *Comput. Struct.*, **77**(6), 711-724.
- Hibbit, Karlsson & Sorensen Inc. (2002). ABAQUS Standard (version 6.3-1).
- Klausbruckner, M. J. and Pryputniewicz, R. J. (1995), "Theoretical and experimental study of coupled vibrations of channel beams", *J. Sound Vib.*, **183**(2), 239-252.
- Ohga, M., Nishimoto, K., Shigematsu, T. and Hara, T. (1998), "Natural frequencies and mode shapes of thin-walled members under in-plane forces", *Thin-Walled Structures – Research and Development*, N. E. Shanmugam, J. Y. R. Liew, V. Thevendran (eds.), Elsevier, 501-508.
- Okamura, M. and Fukasawa, Y. (1998), "Characteristics of instability of local vibration of the thin-walled members under periodic axial forces", *Structural and Earthquake Engineering* (JSCE), **15**(2), 215s-223s.
- Roberts, T. M. (1987), "Natural frequencies of thin-walled bars of open cross-section", *J. Eng. Mech.* ASCE, **113**(10), 1584-1593.
- Schardt, R. (1989), *Verallgemeinerte Technische Biegetheorie*, Springer-Verlag. (German)
- Schardt, R. (1994), "Generalised beam theory - An adequate method for coupled stability problems", *Thin-Walled Structures*, **19**(2-4), 161-180.
- Schardt, R. and Heinz, D. (1991), "Vibrations of thin-walled prismatic structures under simultaneous static load using generalized beam theory", *Structural Dynamics*, W. B. Krätzig *et al.* (eds.), Balkema, Rotterdam, 921-927.
- Silvestre, N. (2005), "Generalised Beam Theory: New formulations, numerical implementation and applications", Ph.D. Thesis, Civil Engineering Department, IST, Technical University of Lisbon. (Portuguese)
- Silvestre, N. and Camotim, D. (2003), "Buckling and vibration behaviour of cold-formed steel members: A comparative study", *Proc. of IV Congress on Steel and Composite Construction* (Lisbon, December 4-5) A. Lamas *et al.* (eds.), 355-365. (Portuguese)
- Silvestre, N. and Camotim, D. (2005a), "Generalized Beam Theory to analyse the vibration behaviour of loaded thin-walled members", *CD-ROM Proc. of the 3rd Int. Conf. on Structural Stability and Dynamics* (ICSSD 2005-Kissimmee, Florida, June 19-22).
- Silvestre, N. and Camotim, D. (2005b), "Local and global vibration behaviour of loaded folded-plate anisotropic members", *Programme and Book of Abstracts of the 12th Int. Congress on Sound and Vibration* (ICSV12-Lisbon, July 11-14), 191-192. (full paper in CD-ROM proceedings - paper 604)
- Silvestre, N. and Camotim, D. (2006), "GBT-Based local and global vibration analysis of loaded composite open-section thin-walled members", *Int. J. Structural Stability and Dynamics*, **6**(1), 1-29.
- Wittrick, W. H. (1985), "Some observations on the dynamic equations of prismatic members in compression", *Int. J. of Mechanical Sciences*, **27**(6), 375-382.